



Published in final edited form as:

J Immunol. 2016 January 15; 196(2): 573–585. doi:10.4049/jimmunol.1501406.

Selective ORAI1 inhibition ameliorates autoimmune CNS inflammation by suppressing effector but not regulatory T cell function

Ulrike Kaufmann*, Patrick J. Shaw*, Lina Kozhaya‡, Raju Subramanian§, Kevin Gaida†, Derya Unutmaz‡,1, Helen J. McBride#, and Stefan Feske*

*Department of Pathology, New York University School of Medicine, New York, NY 10016, USA

‡Department of Microbiology, New York University School of Medicine, New York, NY 10016, USA

§Pharmacokinetics and Drug Metabolism, Amgen, Inc. Thousand Oaks, CA 91320, USA

†Inflammation Research, Amgen, Inc. Thousand Oaks, CA 91320, USA

#Comparative Biology and Safety Sciences, Amgen, Inc. Thousand Oaks, CA 91320, USA

Abstract

The function of CD4⁺ T cells is dependent on Ca²⁺ influx through Ca²⁺ release-activated Ca²⁺ (CRAC) channels formed by ORAI proteins. To investigate the role of ORAI1 in pro-inflammatory Th1 and Th17 cells and autoimmune diseases, we genetically and pharmacologically modulated ORAI1 function. Immunization of mice lacking *Orai1* in T cells with MOG peptide resulted in attenuated severity of experimental autoimmune encephalomyelitis (EAE). The numbers of T cells and innate immune cells in the CNS of ORAI1-deficient animals were strongly reduced along with almost completely abolished production of IL-17, IFN- γ and GM-CSF despite only partially reduced Ca²⁺ influx. In Th1 and Th17 cells differentiated in vitro, ORAI1 was required for cytokine production but not the expression of Th1- and Th17-specific transcription factors T-bet and ROR γ t. The differentiation and function of induced iTreg cells, by contrast, was independent of ORAI1. Importantly, induced genetic deletion of *Orai1* in adoptively transferred, MOG-specific T cells was able to halt EAE progression after disease onset. Likewise, treatment of wild-type mice with a selective CRAC channel inhibitor after EAE onset ameliorated disease. Genetic deletion of *Orai1* and pharmacological ORAI1 inhibition reduced the leukocyte numbers in the CNS and attenuated Th1/Th17 cell-mediated cytokine production. In human CD4⁺ T cells, CRAC channel inhibition reduced the expression of IL-17, IFN- γ and other cytokines in a dose-dependent manner. Taken together, these findings support the conclusion that Th1 and Th17 cell function is particularly dependent on CRAC channels, which could be exploited as a therapeutic approach to T cell-mediated autoimmune diseases.

Address Correspondence to: Stefan Feske, MD, Department of Pathology, Experimental Pathology Program, New York University School of Medicine, 550 First Avenue, Smilow 316, New York, NY 10016, Tel: (212) 263-9066, Fax: (212) 263 8211, feskes01@nyumc.org.

¹Current address: The Jackson Laboratory for Genomic Medicine, Farmington, CT 06032, USA

Conflict of interest statement: S.F. is a cofounder of Calcimedica; R.S., K.G., and H.J.M are full-time employees of Amgen, Inc.; The remaining authors (U.K., P.J.S., L.K. and D.U.) declare no conflict of interest.

Keywords

ORAI1; CRAC channels; SOCE; Th1; Th17; EAE; Multiple sclerosis

Introduction

Tissue specific autoimmune diseases, such as multiple sclerosis (MS), generally result from a breakdown of peripheral immune tolerance to self-antigens, which leads to priming and expansion of self-reactive effector T cell populations that mediate autoimmune disease. The mechanisms causing MS have been studied in experimental autoimmune encephalomyelitis (EAE), an animal model in rodents where the disease can be induced by immunization with self-peptides derived from myelin oligodendrocyte glycoprotein (MOG) or by adoptive transfer of autoreactive T cells specific for the peptide (1). Both MS and EAE are defined by inflammation and demyelination of the CNS, leading to neurological deficits such as paralysis of the extremities. Inflammation is mediated by autoreactive T helper cells, which secrete inflammatory cytokines such as IFN- γ , IL-17 and GM-CSF and recruit additional inflammatory cells to the CNS (2).

For several years, IFN- γ producing Th1 cells were thought to be the pathogenic cell type inducing EAE (3). CD4⁺ T cells differentiate into Th1 cells in response to IL-12 stimulation and produce IFN- γ as their signature cytokine, and IFN- γ has been detected in lesions of MS patients (4). More recently, IL-17 expressing Th17 cells were described as an additional pathogenic Th subset in EAE and other autoimmune diseases (5). Th17 cells express the transcription factor ROR γ t that, together with the cytokines TGF- β and IL-6, is required for their differentiation (6, 7). The expansion and maintenance of Th17 cells requires additional cytokine signals through IL-21 and IL-23 signaling (8). More recently, GM-CSF producing Th cells were shown to be important mediators of CNS inflammation in EAE (9). Although GM-CSF is induced by ROR γ t and IL-23, both pathogenic subsets of Th1 and Th17 cells express GM-CSF in vivo (10). So far, it is not fully understood which of the effector T cell populations is the primary pathogenic population or if a combination of subsets contributes to disease severity and/or progression. The high plasticity between these effector T cell populations and the co-expression of the different cytokines complicates efforts to investigate this question. Besides effector T cells, Foxp3 expressing regulatory T cells (Treg) are also involved in autoimmune diseases. Defective regulatory T cell responses lead to breakdown of immunological tolerance and to induction of autoimmune responses (11). An important role for Treg cells in the EAE model has been described in several studies. Whereas adoptive transfer of Treg cells ameliorates autoreactive immune responses during active EAE (12, 13), depletion of Treg cells by injection of anti-CD25 antibodies exacerbates EAE (14).

TCR stimulation results in Ca²⁺ influx through CRAC channels, which is required for the activation of all subsets of CD4⁺ Th cells (15, 16), including the ones described above. Antigen binding to the TCR results in activation of PLC γ 1, production of IP₃ and opening of IP₃ receptor channels in the membrane of the endoplasmic reticulum (ER). The subsequent release Ca²⁺ from the ER is sensed by stromal interaction molecule (STIM) 1 (17), resulting

in its activation and the opening of CRAC channels in the plasma membrane. Ca^{2+} influx through CRAC channels is called store-operated calcium entry (SOCE) because it is regulated by the filling state of ER Ca^{2+} stores. CRAC channels are formed by 3 proteins of the ORAI family, which constitute the ion channel pore (18). In human T cells, ORAI1 is the predominant ORAI homologue mediating SOCE and null mutations of *ORAI1* in human patients abolishes SOCE (18). In mouse T cells, deletion of *Orai1* or substitution with a loss-of-function mutant results in a partial reduction of SOCE and impairs T cell function in vitro and in vivo (19, 20). Ca^{2+} influx through CRAC channels functions as a second messenger and activates Ca^{2+} sensitive signal transduction molecules such as the phosphatase calcineurin and transcription factors like NFAT. NFAT regulates the differentiation and function of multiple subsets of T cells including expression of many cytokine genes (21, 22). Inhibitors of Ca^{2+} dependent signaling pathways such as the calcineurin inhibitors cyclosporin A and tacrolimus are used for the treatment of autoimmune diseases and transplant rejection (23, 24). Cyclosporine provides clinical benefit, but the toxicity profile limits its broad use (25). ORAI1 is a potential target for therapeutic inhibition of T cell-mediated autoimmunity, because it is a crucial signaling component required for T cell activation and function.

In this study, we demonstrate that genetic deletion of the *Orai1* gene in T cells and pharmacological inhibition of ORAI1 inhibits Ca^{2+} influx and the function of pro-inflammatory Th1 and Th17 cells, but not iTreg cells. *Orai1* gene deletion in T cells ameliorated the severity of EAE and the pharmacological inhibition of CRAC channels halted EAE disease progression. The CRAC channel inhibitor also suppressed Ca^{2+} influx and cytokine expression in human T cells. Our findings support the conclusion that Th1 and Th17 cells require CRAC channels for their proper function, whereas iTreg cells are less dependent on this pathway, thus providing a rationale for exploring CRAC channel inhibition as a therapeutic approach in Th1/Th17-mediated autoimmune diseases.

Materials and Methods

Mice

The generation of *Orai1^{fl/fl}* mice (26) and *Stim1^{fl/fl}* mice (27) has been described before. These mice were crossed to *Cd4-Cre* and *Cre-ERT2* mice (Jackson Laboratory [JAX] strains 017336 and 008085). CD45.1 mice were purchased from JAX. Sex-matched male and female mice were used between 6–8 weeks of age and were cared in accordance with the Guide for the Care and Use of Laboratory Animals (28). Mice were group housed in sterile ventilated micro-isolator cages on corn cob bedding in an AAALAC accredited facility. All research protocols were approved by the Institutional Animal Care and Use Committee (NYU Langone Medical Center, New York, NY). Animals had *ad libitum* access to pelleted feed (Purina 5053, Pico Lab Rodent Diet) and water (5 micron filtration and acidified to pH 2.5–2.9) via water bottle. Animals were maintained on a 12:12 hour light:dark cycle in rooms at 68–79 F with 30–70% humidity. All animals were determined specific pathogen free.

Active and passive EAE

Active EAE was induced as described (29). Briefly, mice were immunized s. c. with 200 µg MOG₃₅₋₅₅ peptide (Anaspec) emulsified in complete Freund's adjuvant (CFA) (Difco). On day 0 and day 2, mice were injected intraperitoneally (i.p.) with 200 ng pertussis toxin (List Biological Laboratories). To induce passive EAE, mice were first immunized with MOG₃₅₋₅₅ peptide using the protocol for active EAE. On day 12 after EAE induction, cells were isolated from spleen and lymph nodes and stimulated in vitro with 50 µg/ml MOG₃₅₋₅₅ peptide in the presence of 10 ng/ml recombinant IL-23 (eBioscience) for 3 days. Live cells were isolated by Percoll gradient centrifugation and 4×10^6 cells in 100 µl volume were transferred intravenously (i.v.) by retro-orbital injection into sublethally irradiated CD45.1 recipient mice. On day 0 and day 2 after T cell transfer, recipient mice were injected with 200 ng pertussis toxin i.p. (30). The severity of EAE was scored according to the following clinical scoring system: 0 = no disease; 0.5 = partially limp tail; 1 = paralyzed tail; 2 = hind limb weakness; 3 = hind limb paralysis; 3.5 = hind limb paralysis and hunched back; 4 = hind and fore limb paralysis; 5 = moribundity and death (29). All animals were supported with nutrigel and food on the floor. Mice were euthanized when they lost more than 20% of their original body weight, showed hind and fore limb paralysis or were unable to feed or drink. At the end of the experiment, cells were isolated from the spinal cord (CNS) and spleen of mice and analyzed by flow cytometry.

Histology

Spinal cords of MOG-immunized mice were imbedded in paraffin and serial sections were cut at 5 µm. Slides were stained with hematoxylin and eosin (Thermo Scientific) and 0.1% Luxol fast blue (Acros Organics) in 95% ethanol using standard methods. Images were acquired using a SCN400 slide scanner (Leica) and viewed by Slidepath Digital Image Hub (Leica).

Leukocytes isolation from the CNS

Mice were perfused intracardially with 2 mM EDTA in PBS. The spinal cord was isolated and digested with 4 mg/ml collagenase type I for 45 min at 37°C. Tissues were passed through a 70-µm cell strainer and mononuclear cells were isolated by Percoll gradient centrifugation.

Inducible deletion of loxP-flanked genes by tamoxifen treatment

Gene deletion in adoptively transferred T cells from *Orai1^{fl/fl} Cre-ERT2* and *Stim1^{fl/fl} Cre-ERT2* mice was performed as described previously (31). Briefly, tamoxifen (Sigma) was dissolved in corn oil and 1 mg tamoxifen / 25 g body weight was injected i.p. for 5 consecutive days. As vehicle control, control mice were injected with the same volume of corn oil.

Treatment with CRAC channel inhibitor AMG1

AMG1 (N-(5-(2-chloro-5-(trifluoromethyl)phenyl)-2-pyrazinyl)-2,6-difluorobenzamid) is a selective inhibitor of the CRAC channel synthesized by Amgen that is in the same chemical series as Synta 66 (32, 33) and is described in patents WO2006081391 A2 and

US2006/002874. For in vivo administration, active EAE was induced in WT mice by immunization with MOG₃₅₋₅₅ peptide in CFA. When average clinical EAE scores reached 1, mice were treated with 6 mg/kg of AMG1 formulated in 20% hydroxypropyl beta-cyclodextrin (HPBCD), 1% hydroxypropyl methyl cellulose (HPMC), 1% pluronic F68 pH 2 by oral gavage daily for 10 consecutive days. Littermate control mice were treated with vehicle (20% HPBCD, 1% HPMC, 1% pluronic F68 pH 2) only. For in vitro administration of AMG1, the inhibitor was dissolved in DMSO at 10 mM concentration and added at different concentrations to the cell culture medium as indicated. The final concentration of DMSO in the medium was 100 nM or 1000 nM. AMG1 was added either during Th cell differentiation for 3 consecutive days or at the end of Th cell differentiation before restimulation of Th cells to analyze cytokine production. For intracellular Ca²⁺ measurements, the inhibitor was added 15 min before the start of the experiment.

T cell isolation and differentiation in vitro

CD4⁺ T cells were isolated from single-cell suspensions of spleens and lymph nodes and purified by negative separation with magnetic beads (Stemcell). For in vitro differentiation into Th1, Th17 and iTreg cells, CD4⁺ T cells were stimulated with hamster anti-CD3 and hamster anti-CD28 together with 10 ng/ml IL-12 (Peprotech) and 2 µg/ml anti-IL-4 (eBioscience) for Th1, 20 ng/ml IL-6 (Peprotech), 0.5 ng/ml human TGF-β1 (Peprotech), 2 µg/ml anti-IL-4 and 2 µg/ml anti-IFN-γ (eBioscience) for Th17 and 2.5 ng/ml TGF-β for iTreg cells in IMDM medium (Cellgro) containing 2 mM L-Glutamine, 50 µM β-mercaptoethanol, 100 U/ml penicillin, 100 µg/ml streptomycin and 10% FCS in anti-hamster IgG coated plates for 3 days.

Flow cytometry and intracellular cytokine staining

For analysis of cytokine production, cells were restimulated with 20 nM phorbol 12-myristate 13-acetate (PMA) (Calbiochem) and 1 µM ionomycin (Invitrogen) in the presence of 5 µM brefeldin A for 6 h. Cells were stained with the following antibodies against cell surface markers (all from eBioscience unless otherwise indicated): anti-CD4 (GK1.5), anti-CD45.2 (104), anti-CD8 (53-6.7), anti-CD11b (M1/70), anti-CD11c (N418), anti-Gr-1 (RB6-8C5), anti-TGF-β (TW7-16B4; Biolegend). Cells were fixed and permeabilized with either IC Fix Buffer (eBioscience) for intracellular cytokine staining or Foxp3 Fix Buffer (BioLegend) for Foxp3 staining using the following antibodies (all from eBioscience): anti-IFN-γ (XMG1.2), anti-IL-17 (eBio17B7), anti-GM-CSF (MP1-22E9), anti-IL-10 (JES5-16E3), anti-RORγt (B2D), anti-T-bet (eBio4B10) and anti-Foxp3 (FJK-16s). Cells were analyzed using a LSRII flow cytometer (BD Biosciences) and FlowJo software (Tree Star).

Quantitative real-time PCR

RNA was isolated from CD4⁺ T cells using RNeasy Midi Kit (Qiagen) and cDNA was synthesized using iScript reverse transcriptase (BioRad). cDNAs were amplified with gene-specific primers (*Orai1*: forward GCTCCCTGGTCAGCCATAAG, reverse GCCCGGTGTTAGAGAATGGT; *Rorc*: forward GACAGGGAGCCAAGTTCTCA, reverse CTTGTCCCCACAGATCTTGCA; *Tbx21*: forward

ACTAAGCAAGGACGGCGAAT, reverse TAATGGCTTGTGGGCTCCAG; *Hprt1*: forward AGCCTAAGATGAGCGCAAGT, reverse TTAGGAGGATGGCCACA; *Cd4* forward CAAGCGCCTAAGAGAGATGG, reverse CACCTGTGCAAGAAGCAGAG) using SYBR green master mix (Thermo Fisher Scientific) and a thermal cycler C1000 touch (BioRad). C_T values were normalized to *Hprt1*. Real-time PCR was performed in triplicates.

Intracellular Ca^{2+} measurements

Cells were labeled with 2 μ M Fura-2 AM (Life Technologies) for 30 min in cell culture medium. Cells were attached for 10 min to 96 well imaging plates (Fisher) that were coated with 0.01% (w/v) poly-L-lysine (Sigma) diluted in water for 2 h and then washed with sterile water. Intracellular Ca^{2+} measurements were performed using a Flexstation 3 fluorescence plate reader (Molecular Devices). T cells were stimulated with 1 μ M thapsigargin (EMD Millipore) in Ca^{2+} -free Ringer solution (155 mM NaCl, 4.5 mM KCl, 3 mM $MgCl_2$, 10 mM D-glucose, and 5 mM Na-HEPES) followed by addition of 1 mM Ca^{2+} Ringer solution to induce SOCE. For stimulation by TCR crosslinking, T cells were incubated with 1 μ g/ml Biotin-conjugated anti-CD3 ϵ antibody (145-2C11, BD Biosciences) at the time of Fura-2 loading and stimulated by addition of 1 μ g/ml Streptavidin (Invitrogen), followed by addition of 1 mM Ca^{2+} Ringer solution and in some experiments 0.3 μ M ionomycin. Fura-2 fluorescence emission ratios (F340/380) were collected at 510 nm following excitation at 340 nm and 380 nm every 5 s. Ca^{2+} signals were quantified by analyzing the peak value of F340/380 ratios, the influx rate (F340/380 / s) and the integrated Ca^{2+} signal (area under the curve) after re-addition of Ca^{2+} Ringer solution using GraphPad Prism 6.0 software.

Treg cell suppression assay

Induced Treg (iTreg) cells were differentiated from naïve $CD4^+$ T cells isolated from WT and *Orai1^{fl/fl} Cd4-Cre* mice as described above and rested overnight in culture medium at 37°C. $CD4^+$ effector T cells were isolated from the spleens of WT $CD45.1$ mice, labeled with 5 μ M CFSE (Invitrogen) and stimulated with 1 μ g/ml anti-CD3. iTreg and effector T cells were co-incubated at different ratios (1:8, 1:4, 1:2, 1:1 and 2:1) in 96 well plates. Stimulated effector T cells cultured without iTreg cells were used as positive control. Proliferation of CFSE labeled $CD45.1^+ CD4^+$ effector T cells was assessed after 3 days by flow cytometry.

Human T cell culture and cytokine production

Cytokine production by human T cells was tested using two approaches. First, peripheral blood mononuclear cells (PBMCs) from healthy individuals (New York Blood Center, New York, NY) were prepared using Ficoll-paque plus (GE Amersham). $CD4^+$ T cells were isolated using Dynal $CD4$ Positive Isolation Kit (Invitrogen) directly from purified PBMCs and were >99% pure. $CD4^+$ T cells were sorted by FACS ARIA cell sorter (BD Biosciences) into $CD45RO^+CCR6^+$ and $CD45RO^+CCR6^-$. $CCR6^+$ cells were activated with anti-CD3 and anti-CD28 coated beads (Invitrogen) and expanded in IL-2-containing RPMI 1640 medium for 12 days. For analysis of cytokine production, cells were plated in 96 well plates and stimulated with 40 ng/ml PMA and 500 ng/ml ionomycin for 4 h in the presence

of GolgiStop (BD Biosciences). Cells were pretreated with 100 nM or 1000 nM of AMG1 or the same volume of DMSO as negative control for 1 h before stimulation. Stimulated cells were washed with PBS and stained with Fixable Viability Dye eFluor 506 (eBioscience) to gate on live cells. Cells were then fixed and permeabilized by commercially available Foxp3 intracellular staining kit (eBioscience) and stained intracellularly with antibodies against IL-2 (clone MQ1-17H12), IL-4 (clone MP4-25D2), IL-17 (clone BL168), IFN- γ (clone 4S.B3) and GM-CSF (clone BVD2-21C11) and analyzed by flow cytometry on LSRII instrument (BD Biosciences). Data analyses were done using Flowjo software (Treestar).

Second, human whole blood was obtained from healthy, non-medicated donors in heparin vacutainers. 100 μ l blood was pre-incubated with various concentrations of AMG1 or media for 1 h prior to addition of PMA/ionomycin (Sigma) in 96-well polystyrene flat bottom microtiter tissue culture plates. All reagents were prepared in RPMI 1640 (Invitrogen) plus 10% human serum AB (Gemini Bio-Products) plus 1x PSG (penicillin, streptomycin, glutamine mixture; Invitrogen). The final concentration of whole blood was 50%. The final concentrations of AMG1 ranged from 0.5 nM to 10 μ M. The final concentrations of PMA and ionomycin were 25 ng/mL and 1 μ g/mL, respectively. After 24 h at 37°C, supernatants were collected for cytokine analysis. IL-2, IL-17, TNF α , and IFN- γ levels in the supernatants were determined using an electrochemiluminescent immunoassay from Meso Scale Discovery (MSD). MSD Multi-Spot custom plates were pre-coated with human IL-2, IL-17, TNF α , and IFN- γ capture antibodies. The plates were blocked by addition of 150 μ l MSD HSC assay diluent, incubated for 2 h at room temperature, and each well was washed three times (200 μ l/wash) with PBS containing 0.05% Tween-20. 25 μ l of supernatants were added to the wells and the plates were incubated for 1 h at room temperature with rigorous shaking. A cocktail of human IL-2, IL-17, TNF α , and IFN- γ detection antibodies was diluted to 1 μ g/ml in MSD Ab diluent, and 25 μ l were added to all test wells. Plates were incubated for 1 h at room temperature in the dark with rigorous shaking. The plates were washed with PBS and 150 μ l 2x MSD Read Buffer T (diluted with deionized water), were added to each well. Electrochemiluminescence was measured using an MSD SECTOR HTS Imager.

T cell recall response in vitro

Mice were immunized s.c. with 200 μ g MOG₃₅₋₅₅ peptide (Anaspec) emulsified in complete Freund's adjuvant (CFA) (Difco) without pertussis toxin (PTX). On day 7 after immunization, cells were isolated from spleen and draining lymph nodes and labeled with 5 μ M CFSE (Invitrogen). Cells were stimulated in vitro with different concentrations of MOG₃₅₋₅₅ peptide (0–50 μ g/ml) or 0.5 μ g/ml anti-CD3 and analyzed for CFSE dilution by flow cytometry 3 days later.

Splenocyte Activity Assay

Splenocytes were isolated from the spleens of BALB/c mice. In a 96-well polystyrene round bottom microtiter tissue culture plate, 2×10^5 splenocytes were pre-incubated with various concentrations of AMG1 or media for 0.5 h prior to addition of PMA/ionomycin (Sigma). All reagents were prepared in RPMI 1640 + 10% heat-inactivated FBS + 1X PSG (Invitrogen). The final concentrations of AMG1 ranged from 10 μ M to 0.5 nM. The final

concentrations of PMA and ionomycin were 25 ng/mL and 1 µg/mL, respectively. After 24 h at 37°C, supernatants were collected for cytokine analysis. IL-2 levels in the supernatants were determined using an electrochemiluminescent immunoassay from Meso Scale Discovery (MSD). MSD plates were pre-coated with mouse IL-2 capture antibody. Twenty-five microliters of supernatants were added to the wells and the plates incubated 1 h at room temperature with rigorous shaking. Mouse IL-2 detection antibody was diluted to 1 µg/ml in MSD Ab diluent, and 25 µl were added to all test wells on the plates. Plates were then incubated 1 h at room temperature (protected from light) with rigorous shaking. The plates were then washed three times (200 µl/wash) with PBS containing 0.05% Tween-20, before 150 µl 2X MSD Read Buffer T (diluted with deionized water) was added to each well. Electrochemiluminescence was immediately measured using an MSD SECTOR HTS Imager. The IL-2 IC₅₀ for AMG1 was 6 nM (2.4 ng/mL); and the IL-2 IC₉₀ for AMG1 was 28 nM (11.6 ng/mL) without the correction for protein binding. With the protein binding correction detailed below, the IL-2 IC₅₀ for AMG1 was 1 nM and the IC₉₀ for AMG1 was 5 nM.

Splenocyte Binding Bioanalytical Methods

The free fraction of AMG1 in BALB/c mouse in vitro splenocyte assay was measured by an ultracentrifugation method. 100 nM AMG1 was incubated in splenocyte assay incubation mixture containing 2×10^5 splenocytes for 15 min. Triplicate samples were then centrifuged at 627,000 x g for 3 h at 37°C and the supernatants were analyzed by liquid chromatography-tandem-mass spectrometry (LC-MS/MS). AMG1 concentrations in the supernatant were determined by regression against a standard curve prepared in splenocyte cell culture media (i.e. assay incubation mixture without the splenocytes). The fraction unbound (F_u) was calculated as:

$$F_u = \frac{C_{\text{supernatant}}}{C_{\text{-cell}}},$$

where $C_{\text{supernatant}}$ and C_{cell} are the AMG1 concentrations in the supernatant and splenocyte incubation mixture, respectively.

LC-MS/MS Bioanalytical Methods

Plasma samples from mouse PK studies were prepared for LC-MS/MS analysis by protein precipitation. For analysis of AMG1, calibration standards were prepared in plasma. Eleven calibration concentrations ranging from 0.5 to 5000 ng/mL were prepared by serial dilution of a 100 µg/mL standard in DMSO spiked into control (non-dosed) plasma. A working solution of an internal standard (50 ng/mL) was prepared in acetonitrile (ACN) and added to plasma samples prior to protein precipitation. Plasma protein binding was determined by an ultracentrifugation method (34). Briefly, AMG1 (5 µg/mL) was incubated with mouse plasma for 15 min. Duplicate aliquots were then centrifuged at 627,000 x g for 3 h at 37°C. The ultracentrifugation supernatants and plasma aliquots (in duplicate) were analyzed by LC-MS/MS. AMG1 concentrations in the supernatants and plasma were determined by regression against a standard curve prepared in plasma water (a 30 kDa ultra-filtrate of plasma) or plasma, respectively.

Fraction unbound (F_u) was calculated as:

$$F_u = \frac{C_{\text{supernatant}}}{C_{\text{plasma}}},$$

where $C_{\text{supernatant}}$ and C_{plasma} are the AMG1 concentrations in the supernatants and plasma, respectively. Chromatographic separations were carried out on an ultrahigh-performance LC system (Prominence; Shimadzu Inc., Columbia, MD) with a reverse-phase column (Luna C18(2), 5 μm , 50 by 2.0 mm; Phenomenex Inc., Torrance, CA) maintained at room temperature. The mobile phase consisted of aqueous ammonium acetate (10 mM, pH 5) in 5/95 v/v ACN in water (solvent A) and in 95/5 v/v ACN in water (solvent B). The following solvent gradient conditions were employed at a 0.7 ml/min flow rate: 0 to 0.4 min, 90% A, 0.4 to 1.4 min, 90 to 10% A; 1.4 to 1.9 min, 10% A; 1.9 to 2.0 min, 10 to 90% A; 2.0 to 2.4 min, 90% A. The total run time was 2.5 min. Analyte detection was performed with a multiple reaction mode method in the positive ion mode on a triple quadrupole mass spectrometer (API4000; AB Sciex, Foster City, CA) equipped with a Heated Nebulizer ion source. The monitored multiple reaction transitions were as follows: AMG1 m/z 414.0 \rightarrow m/z 141.2 and reference, m/z 454.2 \rightarrow m/z 200.1. The lower and upper limits of quantitation for AMG1 were 0.5 and 5000 ng/mL, respectively. Bioanalytical data were acquired and processed using the Analyst program (Version 1.5.1; AB Sciex). The MS result tables were exported and the concentrations of AMG1 were then calculated from a standard curve fitted by a weighted ($1/x^2$) linear regression in Watson software (version 7.4; Thermo Fisher Scientific). Non-compartmental analysis was performed within Watson to determine the TK parameters.

Statistical analysis

Statistical analysis of parametric data was performed using either a two-tailed Student's *t* test for comparison of two groups or one-way ANOVA for comparison of more than two conditions. Non-parametric EAE scores were analyzed using the Mann-Whitney test. Differences were considered significant when *p* values were < 0.05 . All graphs show the average \pm SEM.

Results

EAE is ameliorated in mice with T cell-specific deletion of *Orai1*

We generated conditional knockout mice that allow us to investigate the effects of T cell-specific deletion of *Orai1* by crossing *Orai1^{fl/fl}* mice (26) to *Cd4-Cre* and *Cre-ERT2* mice. Deletion of *Orai1* gene expression in CD4⁺ T cells of *Orai1^{fl/fl} Cd4-Cre* mice was validated by quantitative real-time PCR (Figure 1A) and by measuring SOCE (Figure 1B). While *Orai1* mRNA expression was almost completely absent in CD4⁺ T cells from *Orai1^{fl/fl} Cd4-Cre* mice, SOCE following stimulation with the sarcoendoplasmic reticulum ATPase (SERCA) inhibitor thapsigargin (TG) was partially reduced consistent with previous results (19, 20), suggesting that other ORAI homologues contribute to SOCE in ex vivo isolated CD4⁺ T cells. We next examined the importance of ORAI1 for the encephalitogenic function of CD4⁺ T cells by inducing EAE in *Orai1^{fl/fl} Cd4-Cre* and WT control mice by

immunizing mice with MOG₃₅₋₅₅ peptide in CFA. Deletion of *Orail* in CD4⁺ T cells resulted in a comparable incidence and time of onset of EAE compared to littermate controls, but significantly reduced the severity of EAE with lower maximal disease scores (Figure 1C and 1D). Disease scores correlated with extended regions of leukocyte infiltration and demyelination of spinal cord sections in WT mice, which were more pronounced in WT mice compared to *Orail^{fl/fl} Cd4-Cre* mice (Figure 1E). The numbers of CD4⁺ and CD8⁺ T cells infiltrating the CNS of *Orail^{fl/fl} Cd4-Cre* mice were significantly decreased (Figure 1F). This was not due to a defect in the priming of encephalitogenic T cells in the absence of ORAI1 because both WT and *Orail*-deficient CD4⁺ T cells isolated from MOG-immunized mice proliferated equally when restimulated with MOG peptide in vitro (Figure S1A). In contrast to inflammatory T cells, the frequency of Foxp3⁺ Treg cells in the CNS as well as their expression of IL-10 and TGF-β was not impaired (Figure 1G, S2A). In addition to reduced T cells numbers, the infiltration of polymorphonuclear cells (PMN), dendritic cells (DC) and macrophages was significantly attenuated in the CNS of *Orail^{fl/fl} Cd4-Cre* mice (Figure 1H). Importantly, the frequencies of CD4⁺ T cells expressing the inflammatory cytokines IFN-γ, IL-17 and GM-CSF were strongly decreased and almost undetectable in *Orail^{fl/fl} Cd4-Cre* mice compared to WT controls (Figure 1I). These data show that selective deletion of *Orail* in CD4⁺ T cells effectively attenuates EAE severity and prevents infiltration of Th1 and Th17 cells into the CNS despite only partial suppression of SOCE ex vivo.

Functional defect of in vitro differentiated Th1 and Th17 cells, but not Treg cells

We isolated CD4⁺ T cells from *Orail^{fl/fl} Cd4-Cre* and WT mice and differentiated them into Th1, Th17 and iTreg cells for 3 days in vitro to investigate the effects of *Orail* deletion on SOCE and the function of different effector CD4⁺ T cell subsets in more detail. All CD4⁺ T cell subsets showed a strong defect in Ca²⁺ influx after TCR stimulation or with ionomycin (Figure 2A–C). We also tested the expression of signature genes in WT and *Orail*-deficient Th1, Th17 and iTreg cells that were stimulated for 6h with PMA and ionomycin (Th1, Th17 cells) or left unstimulated (iTreg). *Orail*-deficient Th1 cells showed a severe defect in IFN-γ production, and Th17 cells lacking ORAI1 completely failed to produce IL-17 and GM-CSF (Figure 2D, E). This defect could be either due to impaired function or the differentiation of Th1 and Th17 cells. The expression of the transcription factors T-bet and RORγt that are required for the differentiation of Th1 and Th17 cells, respectively, was not significantly reduced in the absence of ORAI1 both at mRNA and protein levels (Figure 2F–I). Similar results were obtained by investigating T-bet and RORγt mRNA expression in lymphocytes isolated from the CNS of MOG-immunized mice that had developed EAE (Figure 2F, G, right panels). Deletion of *Orail* had no effect on the proliferation of Th1, Th17 and iTreg cells differentiated in vitro (Figure S1B, C), which is consistent with normal ex vivo proliferation of MOG-specific CD4⁺ T cells isolated from the spleen and LNs of *Orail*-deficient mice, immunized with MOG-peptide (Figure S1A). Taken together, these data indicate that ORAI1 is necessary for the effector function (i.e. cytokine production), but not the differentiation of Th1 and Th17 cells. To investigate the role of ORAI1 in the differentiation of CD4⁺ T cells into iTreg cells, we measured expression of Foxp3⁺ in CD4⁺ T cells grown under iTreg-polarizing conditions in vitro. The frequency of Foxp3⁺ iTreg cells was comparable in WT and *Orail*-deficient CD4⁺ T cells (Figure 2J). To analyze the

function of ORAI1-deficient iTreg cells, we coincubated WT and *Orai1*-deficient iTreg cells at different ratios with anti-CD3 stimulated CD4⁺ T cells from WT mice (Figure 2K). After 3 days, the frequencies of proliferating WT CD4⁺ T cells were comparable whether they were coincubated with WT or *Orai1*-deficient iTreg cells, indicating that deletion of *Orai1* does not impair the suppressive function of iTreg cells in vitro. Whereas expression of TGF- β was normal in *Orai1*-deficient iTreg cells, that of IL-10 was severely impaired (Figure S2B), although this defect did not seem to affect the suppressive function of iTreg cells (Figure 2K). Collectively, these data demonstrate that whereas ORAI1 mediates TCR-induced Ca²⁺ influx in proinflammatory Th1 and Th17 cells as well as iTreg cells, it is of particular importance for the function of Th1 and Th17, but not iTreg cells.

Induced deletion of *Orai1* in CD4⁺ T cells after EAE onset attenuates CNS inflammation and disease severity

We next evaluated whether ORAI1 is not only required for the initiation of EAE but also to sustain CNS inflammation in EAE. For this purpose, we generated *Orai1^{fl/fl} Cre-ERT2* mice, in which the *Orai1* gene can be inducibly deleted by injection of tamoxifen. Treatment of CD4⁺ T cells from *Orai1^{fl/fl} Cre-ERT2* mice with tamoxifen resulted in significant reduction in *Orai1* mRNA levels and attenuation of SOCE (Figure 3A, B). To test the effects of *Orai1* deletion on EAE progression in vivo, we first immunized *Orai1^{fl/fl} Cre-ERT2* mice with MOG₃₅₋₅₅ peptide in CFA. After EAE had developed, lymphocytes were isolated from their spleen and LNs, stimulated with MOG₃₅₋₅₅ peptide and IL-23 in vitro and transferred to CD45.1⁺ WT mice to passively induce EAE. After the onset of EAE disease symptoms, recipient CD45.1⁺ mice were treated with tamoxifen or vehicle for 5 days to delete *Orai1* selectively in the transferred, MOG-specific CD4⁺ T cells. Tamoxifen treated mice showed a significant reduction of clinical EAE scores compared to mice treated with vehicle alone (Figure 3C). Whereas disease severity progressed in vehicle-treated animals, EAE scores stabilized at lower levels in tamoxifen treated mice. Analysis of cells isolated from the CNS of recipient mice showed reduced numbers of infiltrating CD4⁺ and CD8⁺ T cells in the tamoxifen-treated mice (Figure 3D). Likewise, the numbers of CNS infiltrating macrophages and dendritic cells were significantly lower in these mice compared to controls (Figure 3E). Moreover, the frequencies of CD4⁺ T cells producing IFN- γ or IL-17 were significantly reduced after tamoxifen treatment (Figure 3F). To confirm that the observed suppression of EAE was due to deletion of *Orai1* and not the effects of tamoxifen, we immunized WT mice with MOG₃₅₋₅₅ peptide to induce EAE. After mice developed signs of EAE with an average disease score of 1, we treated animals with tamoxifen or vehicle (corn oil) for 5 consecutive days. Vehicle and tamoxifen-treated WT animals showed a similar course of disease with EAE severity progressively increasing in both cohorts of mice, demonstrating that tamoxifen administration itself has no impact on EAE severity or progression (Figure S3A). Likewise, the expression of IFN- γ , IL-17 and GM-CSF by CD4⁺ T cells in the CNS was comparable between tamoxifen treated WT and control mice (Figure S3B). In the same experiment, tamoxifen treatment of *Orai1^{fl/fl} Cre-ERT2* mice halted EAE progression and reduced IFN- γ , IL-17 and GM-CSF cytokine expression in CD4⁺ T cells from these animals (Figure S3A, B), confirming that the effects of tamoxifen are specific to the deletion of *Orai1*.

To further confirm that the effects of *Orai1* deletion are due to attenuated SOCE, we conducted similar adoptive transfer EAE experiments using *Stim1^{fl/fl} Cre-ERT2* mice (Figure S3C–G). As described above EAE was induced in CD45.1 recipient WT mice by passive transfer of MOG-specific T cells from *Stim1^{fl/fl} Cre-ERT2* mice. Recipient mice were treated with tamoxifen or vehicle for 5 days starting at day 17 after T cell transfer when disease had already progressed and average EAE scores were close to 2. Deletion of *Stim1* at this more advanced stage of disease resulted in significant amelioration of EAE severity (Figure S3C). Whereas EAE scores continued to rise in vehicle-treated mice, loss of *Stim1* halted disease progression and resulted in a decline of EAE scores. The numbers of infiltrating leukocytes were significantly reduced in the CNS of tamoxifen-treated animals compared to vehicle controls (Figure S3D), whereas numbers in the spleen were comparable, suggesting that *Stim1* deletion specifically affects the population of MOG-specific encephalitogenic T cells in the CNS. The numbers of CD4⁺ and CD8⁺ T cells as well as those of macrophages, dendritic cells and neutrophils in the CNS of mice were strongly reduced after *Stim1* deletion (Figure S3E, F). Furthermore, the frequencies of CD4⁺ IFN- γ ⁺ T cells were significantly lower after *Stim1* deletion (Figure S3G). Collectively, these findings demonstrate that attenuation of SOCE in T cells by induced genetic deletion of *Orai1* or *Stim1* has a profound attenuating effect on CNS inflammation during ongoing EAE and the progression of disease.

The CRAC inhibitor AMG1 blocks function of effector but not regulatory T cells in vitro

Induced genetic deletion of *Orai1* and *Stim1* genes should mimic the effects of a selective CRAC channel inhibitor on EAE progression. To examine the therapeutic effects of blocking SOCE on EAE further, we used a novel CRAC inhibitor, AMG1. To investigate the specificity of AMG1, we first compared its effects on SOCE to genetic deletion of *Orai1* in CD4⁺ T cells (Figure S4A–D). Treatment of CD4⁺ T cells with 1 μ M AMG1 attenuated TG-induced peak Ca²⁺ levels to a similar degree as deletion of *Orai1*, but slowed the Ca²⁺ influx rate in WT and *Orai1*-deficient CD4⁺ T cells compared to DMSO-treated cells. Importantly, the integrated cytosolic Ca²⁺ concentrations over time were similar in DMSO-treated *Orai1*-deficient T cells and AMG1-treated WT T cells, suggesting that the drug predominantly inhibits ORAI1-mediated SOCE.

We next investigated the effects of AMG1 on proinflammatory and regulatory T cells in vitro. For this purpose, we differentiated naïve CD4 T cells from WT mice into Th1, Th17 and iTreg cells for 3 days, either in the presence or absence of AMG1, to distinguish between its effects on T cell differentiation and T cell function. When added from the beginning of T cell differentiation, 100 nM AMG1 potently suppressed SOCE following anti-CD3 stimulation in Th1, Th17 and iTreg cells (Figure 4A–C). The effects of AMG1 on SOCE were similar in all three CD4⁺ T cell effector subsets. Suppression was more pronounced in T cells differentiated in vitro compared to freshly isolated CD4⁺ T cells ex vivo (Figure S4A–D), consistent with a stronger ORAI1 dependence of differentiated T cells reported earlier (19, 20) and ORAI1-specific inhibition by AMG1. When AMG1-treated T cells were restimulated in vitro, the frequencies of IFN- γ -producing Th1 cells were significantly reduced compared to DMSO-treated controls, and almost no IL-17-producing Th17 cells could be detected (Figure 4A, B). By contrast, the frequencies of Foxp3⁺ iTreg

cells were comparable. Attenuated IFN- γ and IL-17 levels could be due to defects in the differentiation or function of Th1 and Th17 cells. We therefore evaluated the effects of AMG1 treatment on the function of Th1 and Th17 cells by adding the inhibitor only at the time of restimulation (Figure 4D–F). Acute inhibition of SOCE with AMG1 resulted in strongly reduced SOCE in Th1, Th17 and iTreg cells and significantly attenuated IFN- γ and IL-17 production (Figure 4D–E), respectively, compared to vehicle treated controls. By contrast, addition of the inhibitor for 6h had no effect on the frequency of Foxp3⁺ iTreg cells (Figure 4F). The effects of short-term inhibition by AMG1 on cytokine production were less pronounced compared to those of inhibitor treatment during the entire differentiation and restimulation period, suggesting that SOCE inhibition with AMG1 may not only affect the function of Th1 and Th17 cells but potentially also their differentiation or maintenance.

Progression and severity of EAE are attenuated by treatment of mice with CRAC channel inhibitor

To investigate if pharmacological inhibition of CRAC channels with AMG1 is effective for the treatment of CNS inflammation in EAE, we immunized WT mice with MOG₃₅₋₅₅ peptide. When EAE symptoms reached an average clinical score of 1, mice were treated with 6 mg/kg of AMG1 or vehicle control for 10 days (Figure 5). Pharmacokinetic analysis in a previous study in BALB/c mice showed that mice gavaged orally with 5 mg/kg AMG1 had plasma concentrations between 2–6 nM at 0, 4 and 24 h after administration (Figure S4E), providing IC₉₀ coverage for close to 20 hours as assessed by the inhibitory effects of the compound on stimulated IL-2 production by mouse splenocytes in vitro (data not shown). To ensure 24 h coverage of the IC₉₀ in vivo, 6 mg/kg was selected after PK modeling as an optimal dose. Treatment of mice that had developed EAE scores of 1 with AMG1 for 10 days halted the progression of the disease and stabilized EAE scores. By contrast, disease severity progressed in mice treated with vehicle alone (Figure 5A). Analysis of splenocytes isolated from mice one day after the end of the 10-day treatment period showed significant reduction of Ca²⁺ influx (Figure 5B). It is noteworthy that cells were stimulated ex vivo in the absence of AMG1, suggesting that the inhibitor has prolonged effects on CRAC channel function. The analysis of cells in the CNS showed that inhibitor treatment resulted in significantly reduced infiltration of CD4⁺ cells, dendritic cells and macrophages into the CNS of AMG1-treated mice compared to vehicle-treated control mice (Figure 5C). Although the numbers in Foxp3 expressing Treg cells was reduced, the difference compared to controls was not statistically significant (Figure 5D). Importantly, restimulation of CD4⁺ T cells isolated from the CNS of mice showed profoundly reduced IFN- γ , IL-17 and GM-CSF expression in T cells from AMG1-treated mice compared to control mice even though no inhibitor was added during the 6h restimulation (Figure 5E). Together, these data demonstrate the effectiveness of systemic CRAC channel inhibition for the treatment of ongoing autoimmune CNS inflammation.

Suppression of SOCE and cytokine production in human T cells by CRAC channel inhibitor

Since the CRAC channel inhibitor AMG1 showed remarkable effects on the function of mouse CD4⁺ T cells and EAE progression in mice, we further investigated its impact on human T cells and thereby its potential for application in patients. Human CD4⁺ T cells

from healthy donors were treated for 2h with different concentrations of AMG1 and SOCE was measured after stimulation with TG. The CRAC channel inhibitor blocked SOCE almost completely at concentrations of 100 nM and 1000 nM (Figure 6A). Next, we examined cytokine production by human whole blood from healthy donors stimulated for 24h with PMA and ionomycin. AMG1 suppressed the production of various cytokines in a dose dependent manner with the following IC_{50} 's: 1781 nM (IL-2), 5476 nM (TNF α), 1792 nM (IFN γ), 57 nM (IL-17) (Figure 6B). Of all the cytokines evaluated, IL-17 was the most sensitive to inhibition with AMG1, which is similar to what we had observed in in vitro differentiated CD4⁺ T cells from mice (Figure 4). We next analyzed the effects of AMG1 on cytokine production by human CD4⁺ T cells that had been cultured for 12 days in vitro and were restimulated with PMA and ionomycin in the presence of 100 nM and 1000 nM AMG1. CRAC channel inhibition resulted in a dose-dependent inhibition of the production of IFN- γ , IL-17, GM-CSF, IL-2 and IL-4 (Figure 6C, D). In differentiated human T cells, IL-2 production was most sensitive to inhibition by AMG1. In summary, these data demonstrate that AMG1 is a potent inhibitor of SOCE and cytokine production in human T cells.

Discussion

In this study, we investigated the role of ORAI1 in proinflammatory Th1 and Th17 cell function and CNS inflammation in the EAE model of Multiple Sclerosis. We show that genetic deletion or pharmacological inhibition of ORAI1 in mouse and human CD4⁺ T cells attenuates SOCE and strongly inhibits production of the proinflammatory cytokines IFN- γ , IL17 and GM-CSF. By contrast, no effects were observed on the numbers of Treg cells in CNS lesions or the differentiation and function of iTreg cells in vitro. *Orail* deficiency in mouse CD4⁺ T cells was associated with markedly reduced CNS infiltration of Th1 and Th17 cells and attenuated severity of EAE. Importantly, induced genetic deletion of *Orail* in CD4⁺ T cells or pharmacological inhibition of ORAI1 protein function effectively halted EAE progression and ameliorated disease severity when started after symptoms were established.

We and others have previously shown that indirect inhibition of ORAI channels by deletion of the ER Ca²⁺ sensors STIM1 and STIM2 protects mice from developing EAE after MOG immunization (35, 36). Conditional deletion of *Stim1* or both *Stim1* and *Stim2* in T cells completely prevented EAE, whereas conditional deletion of *Stim2* alone reduced disease severity (35). Similarly, *Stim1*^{-/-} bone marrow chimeras lacking *Stim1* in hematopoietic cells failed to develop EAE, whereas *Stim2*^{-/-} mice showed delayed onset of EAE with a severity of disease that was comparable to WT mice (36). In both studies, MOG-specific T cells lacking STIM1 isolated from the spleen or CNS of mice showed reduced production of IFN- γ , IL-2 and IL-17 when restimulated in vitro. STIM2-deficient T cells showed a similar, but weaker defect in cytokine production (35, 36). Indirect suppression of Ca²⁺ influx by inhibiting the potassium channel Kv1.3 with sea anemone-derived ShK peptides was able to ameliorate EAE induced by adoptive transfer of myelin-specific T cells and chronic-relapsing EAE in rats (37–39). Inhibition of Kv1.3 depolarizes the plasma membrane and reduces the electrical gradient required for Ca²⁺ influx through CRAC channels in T cells (40). More recently, Gwack and colleagues identified inhibitors of CRAC channels that

prevented the development of EAE in mice when administered at the time of EAE induction (41). We show here, for the first time to our knowledge, that inhibition of CRAC channels during established EAE ameliorates CNS inflammation and disease severity. We use several approaches to show the therapeutic benefit of interfering with ORAI1 channel function directly instead of deleting STIM molecules or inhibiting Kv1.3 channels. First, we made use of newly developed *Orai1^{fl/fl} Cd4-Cre* mice with specific deletion of ORAI1 channels in T cells. Second, we inducibly deleted *Orai1* gene expression in adoptively transferred myelin-specific T cells from *Orai1^{fl/fl} Cre-ERT2* mice after they had induced EAE in host mice. Third, we treated WT mice with ongoing EAE with the CRAC channel inhibitor AMG1. Collectively, these data show that interfering with ORAI1 channel function genetically or pharmacologically ameliorates CNS inflammation and EAE by inhibiting proinflammatory Th1 and Th17 cell function and by reducing the numbers of T cells and innate immune cells in the CNS.

Loss-of-function or null mutations in *ORAI1* in human patients abolish SOCE and CRAC channel function in affected CD4⁺ T cells (18, 42, 43). By contrast, CD4⁺ T cells isolated from *Orai1^{fl/fl} Cd4-Cre* mice showed strong residual SOCE despite negligible *Orai1* mRNA expression. The SOCE defect was more pronounced in anti-CD3/CD28-stimulated CD4⁺ T cells cultured under Th1, Th17 and iTreg polarizing conditions in vitro. Ca²⁺ influx in all three effector T cell subsets was strongly reduced after stimulation by TCR crosslinking or store depletion with low-dose ionomycin. These findings suggest that all three effector CD4⁺ T cell subsets predominantly utilize ORAI1 to mediate SOCE, whereas other ORAI homologues, i.e. ORAI2 or ORAI3, likely contribute to SOCE in ex vivo isolated CD4⁺ T cells. These findings are consistent with earlier observations in *Orai1^{-/-}* and *Orai1^{R93W}* knock-in mice that are homozygous for a non-functional *Orai1* allele (19, 20). However, the specific role of ORAI2 and ORAI3 in SOCE in T cells and in T cell-mediated immune responses in mice remains to be investigated.

Despite incomplete inhibition of SOCE, ORAI1-deficient CD4⁺ T cells showed a striking defect in proinflammatory Th1 and Th17 cell function. CD4⁺ T cells isolated from the CNS of MOG-immunized *Orai1^{fl/fl} Cd4-Cre* mice or mice transferred with MOG-specific T cells from *Orai1^{fl/fl} Cre-ERT2* mice had markedly reduced production of IFN- γ , IL-17 and GM-CSF. The defect in proinflammatory cytokine production was most pronounced in CD4⁺ T cells from *Orai1^{fl/fl} Cd4-Cre* mice that were differentiated under Th1 and Th17 polarizing conditions in vitro, which is consistent with their strongly reduced SOCE compared to ex vivo CD4⁺ T cells. These findings suggest that Th1 and in particular Th17 cells require strong SOCE to induce cytokine gene expression. Even moderate reduction of SOCE in freshly isolated CD4⁺ T cells from *Orai1^{fl/fl} Cd4-Cre* mice with EAE suppressed IFN- γ and IL-17 production. This interpretation is in line with our earlier observations that CD4⁺ T cells lacking STIM2 have a marked defect in IL-17 production despite only moderately reduced SOCE, and that MOG-immunized *Stim2^{fl/fl} Cd4-Cre* develop a less severe form of EAE (27, 35).

It is not understood if Ca²⁺ influx through ORAI1 channels is primarily required for effector functions of Th1 and Th17 cells or also affects their differentiation. A recent study showed decreased expression of the Th17-specific transcription factors ROR α and ROR γ t in Th17

cells from *Orai1*^{-/-} mice (41). By contrast, we did not observe reduced mRNA and protein expression of *Rorc* in Th17 cells and *Tbx21* in Th1 cells derived from *Orai1*^{fl/fl} *Cd4-Cre* mice. The cause of this difference is not known, but may be related to different levels of residual SOCE in CD4⁺ T cells from both mouse strains. CD4⁺ T cells from *Stim1*^{fl/fl} *Cd4-Cre* mice that have a more pronounced defect in SOCE than CD4⁺ T cells from *Orai1*^{fl/fl} *Cd4-Cre* mice have partially reduced ROR γ t expression when differentiated into Th17 cells in vitro (UK, SF, unpublished). To distinguish the role of SOCE in Th1 and Th17 differentiation and function, we added the CRAC channel inhibitor AMG1 to CD4⁺ T cells at the beginning of their 3 day-differentiation into Th1 and Th17 cells in vitro and to already differentiated Th1 and Th17 cells. IL-17, but not IFN- γ , production was more strongly reduced in T cells that were cultured in the presence of the inhibitor during the entire differentiation period, which may suggest that SOCE, in addition to its role in Th17 cell function, contributes to the differentiation of Th17 cells. The differentiation of CD4⁺ T cells into encephalitogenic effector Th17 cells requires expression of several cytokine receptors including IL-23R (44–46) and deletion of IL-23R protects mice from EAE (45). We had previously shown that IL-23R expression is reduced in *Stim1*-deficient T cells (35). Thus, while ORAI1 is not critical for ROR γ t expression in our hands, it may nevertheless be required for the terminal differentiation of pathogenic effector Th17 cells.

Impaired cytokine production of ORAI1-deficient Th1 and Th17 cells was in contrast to normal numbers and function of CNS infiltrating Foxp3⁺ Treg cells in the absence of ORAI1. *Orai1*-deficient Treg cells isolated from the CNS showed IL-10 and TGF β expression comparable to WT Treg cells. Likewise, deletion of *Orai1* did not affect the differentiation of iTreg cells in vitro. Naïve CD4⁺ T cells from *Orai1*^{fl/fl} *Cd4-Cre* mice that were polarized into iTreg cells showed similar frequencies of Foxp3⁺ cells, consistent with normal iTreg development of CD4⁺ T cells in the absence of ORAI1 reported earlier (47). Similarly, the CRAC channel inhibitor AMG1 did not interfere with the differentiation of WT CD4⁺ T cells into iTreg cells in vitro. In addition, iTreg cells generated from *Orai1*^{fl/fl} *Cd4-Cre* mice were fully functional and suppressed the proliferation of effector T cells, despite reduced IL-10 expression. A similar reduction of IL-10 expression was not observed in Foxp3⁺ Treg cells isolated from the CNS of MOG-immunized *Orai1*^{fl/fl} *Cd4-Cre* mice, likely because Treg cells in the CNS are mainly nTreg cells that appear to be able to express IL-10 in the absence of ORAI1. Normal suppressive function was also observed in iTreg cells generated from CD4⁺ T cells of *Stim1*^{fl/fl} *Cd4-Cre* mice (48). *Stim1*-deficient CD4⁺ T cells were, however, impaired in their differentiation into Foxp3⁺ iTreg cells in vitro and after adoptive transfer into lymphopenic host mice in vivo (48). The different effects of *Orai1* and *Stim1* deletion on iTreg differentiation are likely due to the more profound SOCE defect in CD4⁺ T cells lacking STIM1 rather than qualitative differences in ORAI1 and STIM1 dependent signal transduction. It is noteworthy that neither *Stim1*^{fl/fl} *Cd4-Cre* nor *Orai1*^{fl/fl} *Cd4-Cre* have reduced numbers of nTreg cells in the thymus or secondary lymphoid organs (27, 47). Only complete suppression of SOCE in T cells of *Stim1*^{fl/fl} *Stim2*^{fl/fl} *Cd4-Cre* mice affects nTreg development (27, 49). From a translational perspective, the selective effects of *Orai1* deletion and the resulting incomplete suppression of SOCE on proinflammatory Th1 and Th17 cells, but not Treg cells, might be advantageous compared to currently used inhibitors of the Ca²⁺/calcineurin/NFAT pathway such as

cyclosporine A, which was shown to also inhibit Foxp3⁺ Treg cells in vitro and in vivo (47, 50, 51).

The CRAC channel inhibitor AMG1 we used in this study effectively suppressed proinflammatory cytokine production by mouse and human CD4⁺ T cells and ameliorated CNS inflammation and EAE symptoms when administered after disease onset. The effectiveness of the inhibitor on CNS inflammation and EAE severity was comparable to the effects of T cell-specific *Orai1* deletion in *Orai1^{fl/fl} Cd4-Cre* mice and tamoxifen-induced deletion of *Orai1* in MOG-specific T cells. The inhibitor also reduced IFN- γ and IL-17 production by Th1 and Th17 cells, respectively, in vitro to a similar degree as genetic *Orai1* deletion. Neither *Orai1* deletion nor the CRAC channel inhibitor significantly affected the differentiation of murine iTreg cells in vitro or the numbers of Treg cells in the CNS of MOG immunized mice. While it is likely that AMG1 also inhibits CRAC channels in other immune cells such as DC, macrophages and neutrophils, this may not result in a functional impairment of these cells and influence EAE severity because we recently showed that even complete suppression of SOCE in *Stim1/Stim2*-deficient DC and macrophages does not significantly impair the function of these cells (52). Given the similar degree of EAE attenuation in mice with genetic deletion of *Orai1* in T cells and WT mice treated with AMG1, the main effects of the inhibitor on EAE are likely to result from inhibition of encephalitogenic T cells. Similar to AMG1, another CRAC channel inhibitor that was recently reported suppressed Th17 cell function and differentiation without affecting iTreg differentiation (41). A less toxic derivative of that compound was able to prevent EAE when administered before onset of the disease; its therapeutic effect on established EAE was not tested. In contrast to that inhibitor (41) and AMG1, CsA and the CRAC channel inhibitor YM-58483 (BTP2) were shown to inhibit the development and function of iTreg cells (47). A possible explanation for this discrepancy lies in the specificities of the inhibitors for different ion channels. BTP2 has established effects on other ion channels that modulate SOCE (53) and CsA is downstream of all Ca²⁺ signaling regardless of the channel involved.

The anti-inflammatory effects of ORAI1 inhibition on Th1 and Th17 cell function and EAE need to be balanced against its potential suppression of immune responses to infection. In this regard it is noteworthy that only complete suppression of SOCE by combined deletion of *Stim1* and *Stim2*, but not incomplete suppression of SOCE by deletion of *Stim1* or *Stim2* alone, negatively affected CD4⁺ and CD8⁺ T cell mediated immune responses to LCMV infection by interfering with the maintenance of memory CD8⁺ T cells and recall responses to infection (54). Likewise, only *Stim1^{fl/fl} Stim2^{fl/fl} Cd4-Cre* but not *Stim1^{fl/fl} Cd4-Cre* mice, showed impaired T cell-dependent antitumor immune responses (55). Taken together, these findings suggest that residual SOCE is sufficient for immunity to infection, and that incomplete pharmacological inhibition of CRAC channels by targeting ORAI1 may selectively inhibit proinflammatory T cells in autoimmune diseases without affecting protective immune responses.

Supplementary Material

Refer to Web version on PubMed Central for supplementary material.

Acknowledgments

This work was funded by NIH grants AI097302 to S.F. and AI065303 to D.U., a postdoctoral fellowship by the Deutsche Forschungsgemeinschaft (DFG) KA 4083/2-1 to U.K. and a postdoctoral fellowship by the National Multiple Sclerosis Society to P.S.

We thank Joel Esmay, Jim Meyer, Valerie Almon (Amgen Inc.) for laboratory support. We also thank members of the Feske lab for helpful discussions.

References

1. Ben-Nun A, Wekerle H, Cohen IR. The rapid isolation of clonable antigen-specific T lymphocyte lines capable of mediating autoimmune encephalomyelitis. *Eur J Immunol.* 1981; 11:195–199. [PubMed: 6165588]
2. Kuchroo VK, Anderson AC, Waldner H, Munder M, Bettelli E, Nicholson LB. T cell response in experimental autoimmune encephalomyelitis (EAE): role of self and cross-reactive antigens in shaping, tuning, and regulating the autopathogenic T cell repertoire. *Annu Rev Immunol.* 2002; 20:101–123. [PubMed: 11861599]
3. Ando DG, Clayton J, Kono D, Urban JL, Sercarz EE. Encephalitogenic T cells in the B10.PL model of experimental allergic encephalomyelitis (EAE) are of the Th-1 lymphokine subtype. *Cell Immunol.* 1989; 124:132–143. [PubMed: 2478300]
4. Traugott U, Lebon P. Interferon-gamma and Ia antigen are present on astrocytes in active chronic multiple sclerosis lesions. *J Neurol Sci.* 1988; 84:257–264. [PubMed: 3132537]
5. Langrish CL, Chen Y, Blumenschein WM, Mattson J, Basham B, Sedgwick JD, McClanahan T, Kastelein RA, Cua DJ. IL-23 drives a pathogenic T cell population that induces autoimmune inflammation. *J Exp Med.* 2005; 201:233–240. [PubMed: 15657292]
6. Veldhoen M, Hocking RJ, Atkins CJ, Locksley RM, Stockinger B. TGFbeta in the context of an inflammatory cytokine milieu supports de novo differentiation of IL-17-producing T cells. *Immunity.* 2006; 24:179–189. [PubMed: 16473830]
7. Bettelli E, Carrier Y, Gao W, Korn T, Strom TB, Oukka M, Weiner HL, Kuchroo VK. Reciprocal developmental pathways for the generation of pathogenic effector TH17 and regulatory T cells. *Nature.* 2006; 441:235–238. [PubMed: 16648838]
8. Zhou L, Ivanov, Spolski R, Min R, Shenderov K, Egawa T, Levy DE, Leonard WJ, Littman DR. IL-6 programs T(H)-17 cell differentiation by promoting sequential engagement of the IL-21 and IL-23 pathways. *Nat Immunol.* 2007; 8:967–974. [PubMed: 17581537]
9. Ponomarev ED, Shriver LP, Maresz K, Pedras-Vasconcelos J, Verthelyi D, Dittel BN. GM-CSF production by autoreactive T cells is required for the activation of microglial cells and the onset of experimental autoimmune encephalomyelitis. *J Immunol.* 2007; 178:39–48. [PubMed: 17182538]
10. Codarri L, Gyulveszi G, Tosevski V, Hesse L, Fontana A, Magnenat L, Suter T, Becher B. RORgamma drives production of the cytokine GM-CSF in helper T cells, which is essential for the effector phase of autoimmune neuroinflammation. *Nat Immunol.* 2011; 12:560–567. [PubMed: 21516112]
11. Wing K, Sakaguchi S. Regulatory T cells exert checks and balances on self tolerance and autoimmunity. *Nat Immunol.* 2010; 11:7–13. [PubMed: 20016504]
12. Kohm AP, Carpentier PA, Anger HA, Miller SD. Cutting edge: CD4+CD25+ regulatory T cells suppress antigen-specific autoreactive immune responses and central nervous system inflammation during active experimental autoimmune encephalomyelitis. *J Immunol.* 2002; 169:4712–4716. [PubMed: 12391178]
13. Stephens LA, Malpass KH, Anderton SM. Curing CNS autoimmune disease with myelin-reactive Foxp3+ Treg. *Eur J Immunol.* 2009; 39:1108–1117. [PubMed: 19350586]
14. Montero E, Nussbaum G, Kaye JF, Perez R, Lage A, Ben-Nun A, Cohen IR. Regulation of experimental autoimmune encephalomyelitis by CD4+, CD25+ and CD8+ T cells: analysis using depleting antibodies. *J Autoimmun.* 2004; 23:1–7. [PubMed: 15236747]
15. Lewis RS. Store-operated calcium channels: new perspectives on mechanism and function. *Cold Spring Harb Perspect Biol.* 2011:3.

16. Feske S. Calcium signalling in lymphocyte activation and disease. *Nat Rev Immunol.* 2007; 7:690–702. [PubMed: 17703229]
17. Liou J, Kim ML, Heo WD, Jones JT, Myers JW, Ferrell JE Jr, Meyer T. STIM is a Ca²⁺ sensor essential for Ca²⁺-store-depletion-triggered Ca²⁺ influx. *Curr Biol.* 2005; 15:1235–1241. [PubMed: 16005298]
18. Feske S, Gwack Y, Prakriya M, Srikanth S, Puppel SH, Tanasa B, Hogan PG, Lewis RS, Daly M, Rao A. A mutation in Orai1 causes immune deficiency by abrogating CRAC channel function. *Nature.* 2006; 441:179–185. [PubMed: 16582901]
19. Gwack Y, Srikanth S, Oh-Hora M, Hogan PG, Lamperti ED, Yamashita M, Gelinis C, Neems DS, Sasaki Y, Feske S, Prakriya M, Rajewsky K, Rao A. Hair loss and defective T- and B-cell function in mice lacking ORAI1. *Mol Cell Biol.* 2008; 28:5209–5222. [PubMed: 18591248]
20. McCarl CA, Khalil S, Ma J, Oh-hora M, Yamashita M, Roether J, Kawasaki T, Jairaman A, Sasaki Y, Prakriya M, Feske S. Store-operated Ca²⁺ entry through ORAI1 is critical for T cell-mediated autoimmunity and allograft rejection. *J Immunol.* 2010; 185:5845–5858. [PubMed: 20956344]
21. Feske S, Giltman J, Dolmetsch R, Staudt LM, Rao A. Gene regulation mediated by calcium signals in T lymphocytes. *Nat Immunol.* 2001; 2:316–324. [PubMed: 11276202]
22. Hermann-Kleiter N, Baier G. NFAT pulls the strings during CD4⁺ T helper cell effector functions. *Blood.* 2010; 115:2989–2997. [PubMed: 20103781]
23. Bierer BE, Hollander G, Fruman D, Burakoff SJ. Cyclosporin A and FK506: molecular mechanisms of immunosuppression and probes for transplantation biology. *Curr Opin Immunol.* 1993; 5:763–773. [PubMed: 7694595]
24. Taylor AL, Watson CJ, Bradley JA. Immunosuppressive agents in solid organ transplantation: Mechanisms of action and therapeutic efficacy. *Crit Rev Oncol Hematol.* 2005; 56:23–46. [PubMed: 16039869]
25. Mihatsch MJ, Kyo M, Morozumi K, Yamaguchi Y, Nickleit V, Ryffel B. The side-effects of ciclosporine-A and tacrolimus. *Clin Nephrol.* 1998; 49:356–363. [PubMed: 9696431]
26. Somasundaram A, Shum AK, McBride HJ, Kessler JA, Feske S, Miller RJ, Prakriya M. Store-operated CRAC channels regulate gene expression and proliferation in neural progenitor cells. *J Neurosci.* 2014; 34:9107–9123. [PubMed: 24990931]
27. Oh-Hora M, Yamashita M, Hogan PG, Sharma S, Lamperti E, Chung W, Prakriya M, Feske S, Rao A. Dual functions for the endoplasmic reticulum calcium sensors STIM1 and STIM2 in T cell activation and tolerance. *Nat Immunol.* 2008; 9:432–443. [PubMed: 18327260]
28. National Research Council (U.S.). Committee for the Update of the Guide for the Care and Use of Laboratory Animals., Institute for Laboratory Animal Research (U.S.), and National Academies Press (U.S.). *Guide for the care and use of laboratory animals.* 8. National Academies Press; Washington, D.C: 2011. p. xxvp. 220
29. Stromnes IM, Goverman JM. Active induction of experimental allergic encephalomyelitis. *Nat Protoc.* 2006; 1:1810–1819. [PubMed: 17487163]
30. Stromnes IM, Goverman JM. Passive induction of experimental allergic encephalomyelitis. *Nat Protoc.* 2006; 1:1952–1960. [PubMed: 17487182]
31. Kuhbandner S, Brummer S, Metzger D, Chambon P, Hofmann F, Feil R. Temporally controlled somatic mutagenesis in smooth muscle. *Genesis.* 2000; 28:15–22. [PubMed: 11020712]
32. Di Sabatino A, Rovedatti L, Kaur R, Spencer JP, Brown JT, Morisset VD, Biancheri P, Leakey NA, Wilde JI, Scott L, Corazza GR, Lee K, Sengupta N, Knowles CH, Gunthorpe MJ, McLean PG, MacDonald TT, Kruidenier L. Targeting gut T cell Ca²⁺ release-activated Ca²⁺ channels inhibits T cell cytokine production and T-box transcription factor T-bet in inflammatory bowel disease. *J Immunol.* 2009; 183:3454–3462. [PubMed: 19648266]
33. van Kruchten R, Braun A, Feijge MA, Kuijpers MJ, Rivera-Galdos R, Kraft P, Stoll G, Kleinschnitz C, Bevers EM, Nieswandt B, Heemskerk JW. Antithrombotic potential of blockers of store-operated calcium channels in platelets. *Arterioscler Thromb Vasc Biol.* 2012; 32:1717–1723. [PubMed: 22580895]
34. Nakai D, Kumamoto K, Sakikawa C, Kosaka T, Tokui T. Evaluation of the protein binding ratio of drugs by a micro-scale ultracentrifugation method. *J Pharm Sci.* 2004; 93:847–854. [PubMed: 14999723]

35. Ma J, McCarl CA, Khalil S, Luthy K, Feske S. T-cell-specific deletion of STIM1 and STIM2 protects mice from EAE by impairing the effector functions of Th1 and Th17 cells. *Eur J Immunol.* 2010; 40:3028–3042. [PubMed: 21061435]
36. Schuhmann MK, Stegner D, Berna-Erro A, Bittner S, Braun A, Kleinschnitz C, Stoll G, Wiendl H, Meuth SG, Nieswandt B. Stromal interaction molecules 1 and 2 are key regulators of autoreactive T cell activation in murine autoimmune central nervous system inflammation. *J Immunol.* 2010; 184:1536–1542. [PubMed: 20028655]
37. Beeton C, Wulff H, Barbaria J, Clot-Faybesse O, Pennington M, Bernard D, Cahalan MD, Chandy KG, Beraud E. Selective blockade of T lymphocyte K(+) channels ameliorates experimental autoimmune encephalomyelitis, a model for multiple sclerosis. *Proceedings of the National Academy of Sciences of the United States of America.* 2001; 98:13942–13947. [PubMed: 11717451]
38. Beeton C, Wulff H, Standifer NE, Azam P, Mullen KM, Pennington MW, Kolski-Andreaco A, Wei E, Grino A, Counts DR, Wang PH, LeeHealey CJ, SAB, Sankaranarayanan A, Homerick D, Roeck WW, Tehranzadeh J, Stanhope KL, Zimin P, Havel PJ, Griffey S, Knaus HG, Nepom GT, Gutman GA, Calabresi PA, Chandy KG. Kv1.3 channels are a therapeutic target for T cell-mediated autoimmune diseases. *Proceedings of the National Academy of Sciences of the United States of America.* 2006; 103:17414–17419. [PubMed: 17088564]
39. Tarcha EJ, Chi V, Munoz-Elias EJ, Bailey D, Londono LM, Upadhyay SK, Norton K, Banks A, Tjong I, Nguyen H, Hu X, Ruppert GW, Boley SE, Slaughter R, Sams J, Knapp B, Kentala D, Hansen Z, Pennington MW, Beeton C, Chandy KG, Iadonato SP. Durable pharmacological responses from the peptide ShK-186, a specific Kv1.3 channel inhibitor that suppresses T cell mediators of autoimmune disease. *The Journal of pharmacology and experimental therapeutics.* 2012; 342:642–653. [PubMed: 22637724]
40. Feske S, Wulff H, Skolnik EY. Ion channels in innate and adaptive immunity. *Annu Rev Immunol.* 2015; 33:291–353. [PubMed: 25861976]
41. Kim KD, Srikanth S, Tan YV, Yee MK, Jew M, Damoiseaux R, Jung ME, Shimizu S, An DS, Ribalet B, Waschek JA, Gwack Y. Calcium signaling via Orai1 is essential for induction of the nuclear orphan receptor pathway to drive Th17 differentiation. *J Immunol.* 2014; 192:110–122. [PubMed: 24307733]
42. Feske S, Prakriya M, Rao A, Lewis RS. A severe defect in CRAC Ca²⁺ channel activation and altered K⁺ channel gating in T cells from immunodeficient patients. *J Exp Med.* 2005; 202:651–662. [PubMed: 16147976]
43. McCarl CA, Picard C, Khalil S, Kawasaki T, Rother J, Papolos A, Kutok J, Hivroz C, Ledest F, Plogmann K, Ehl S, Notheis G, Albert MH, Belohradsky BH, Kirschner J, Rao A, Fischer A, Feske S. ORAI1 deficiency and lack of store-operated Ca²⁺ entry cause immunodeficiency, myopathy, and ectodermal dysplasia. *The Journal of allergy and clinical immunology.* 2009; 124:1311–1318 e1317. [PubMed: 20004786]
44. Bettelli E, Korn T, Oukka M, Kuchroo VK. Induction and effector functions of T(H)17 cells. *Nature.* 2008; 453:1051–1057. [PubMed: 18563156]
45. McGeachy MJ, Chen Y, Tato CM, Laurence A, Joyce-Shaikh B, Blumenschein WM, McClanahan TK, O’Shea JJ, Cua DJ. The interleukin 23 receptor is essential for the terminal differentiation of interleukin 17-producing effector T helper cells in vivo. *Nat Immunol.* 2009; 10:314–324. [PubMed: 19182808]
46. Cua DJ, Sherlock J, Chen Y, Murphy CA, Joyce B, Seymour B, Lucian L, To W, Kwan S, Churakova T, Zurawski S, Wiekowski M, Lira SA, Gorman D, Kastelein RA, Sedgwick JD. Interleukin-23 rather than interleukin-12 is the critical cytokine for autoimmune inflammation of the brain. *Nature.* 2003; 421:744–748. [PubMed: 12610626]
47. Jin S, Chin J, Kitson C, Woods J, Majmudar R, Carvajal V, Allard J, Demartino J, Narula S, Thomas-Karyat DA. Natural regulatory T cells are resistant to calcium release-activated calcium (CRAC/ORAI) channel inhibition. *Int Immunol.* 2013; 25:497–506. [PubMed: 23667148]
48. Desvignes L, Weidinger C, Shaw P, Vaeth M, Ribierre T, Liu M, Fergus T, Kozhaya L, McVoy L, Unutmaz D, Ernst JD, Feske S. STIM1 controls T cell-mediated immune regulation and inflammation in chronic infection. *J Clin Invest.* 2015

49. Oh-Hora M, Komatsu N, Pishyareh M, Feske S, Hori S, Taniguchi M, Rao A, Takayanagi H. Agonist-selected T cell development requires strong T cell receptor signaling and store-operated calcium entry. *Immunity*. 2013; 38:881–895. [PubMed: 23499491]
50. Coenen JJ, Koenen HJ, van Rijssen E, Hilbrands LB, Joosten I. Rapamycin, and not cyclosporin A, preserves the highly suppressive CD27+ subset of human CD4+CD25+ regulatory T cells. *Blood*. 2006; 107:1018–1023. [PubMed: 16210336]
51. Gao W, Lu Y, El Essawy B, Oukka M, Kuchroo VK, Strom TB. Contrasting effects of cyclosporine and rapamycin in de novo generation of alloantigen-specific regulatory T cells. *American journal of transplantation : official journal of the American Society of Transplantation and the American Society of Transplant Surgeons*. 2007; 7:1722–1732.
52. Vaeth M, Zee I, Concepcion AR, Maus M, Shaw P, Portal-Celhay C, Zahra A, Kozhaya L, Weidinger C, Philips J, Unutmaz D, Feske S. Ca²⁺ Signaling but Not Store-Operated Ca²⁺ Entry Is Required for the Function of Macrophages and Dendritic Cells. *J Immunol*. 2015; 195:1202–1217. [PubMed: 26109647]
53. Takezawa R, Cheng H, Beck A, Ishikawa J, Launay P, Kubota H, Kinet JP, Fleig A, Yamada T, Penner R. A pyrazole derivative potently inhibits lymphocyte Ca²⁺ influx and cytokine production by facilitating transient receptor potential melastatin 4 channel activity. *Molecular pharmacology*. 2006; 69:1413–1420. [PubMed: 16407466]
54. Shaw PJ, Weidinger C, Vaeth M, Luethy K, Kaech SM, Feske S. CD4(+) and CD8(+) T cell-dependent antiviral immunity requires STIM1 and STIM2. *J Clin Invest*. 2014; 124:4549–4563. [PubMed: 25157823]
55. Weidinger C, Shaw PJ, Feske S. STIM1 and STIM2-mediated Ca²⁺ influx regulates antitumour immunity by CD8+ T cells. *EMBO molecular medicine*. 2013; 5:1311–1321. [PubMed: 23922331]

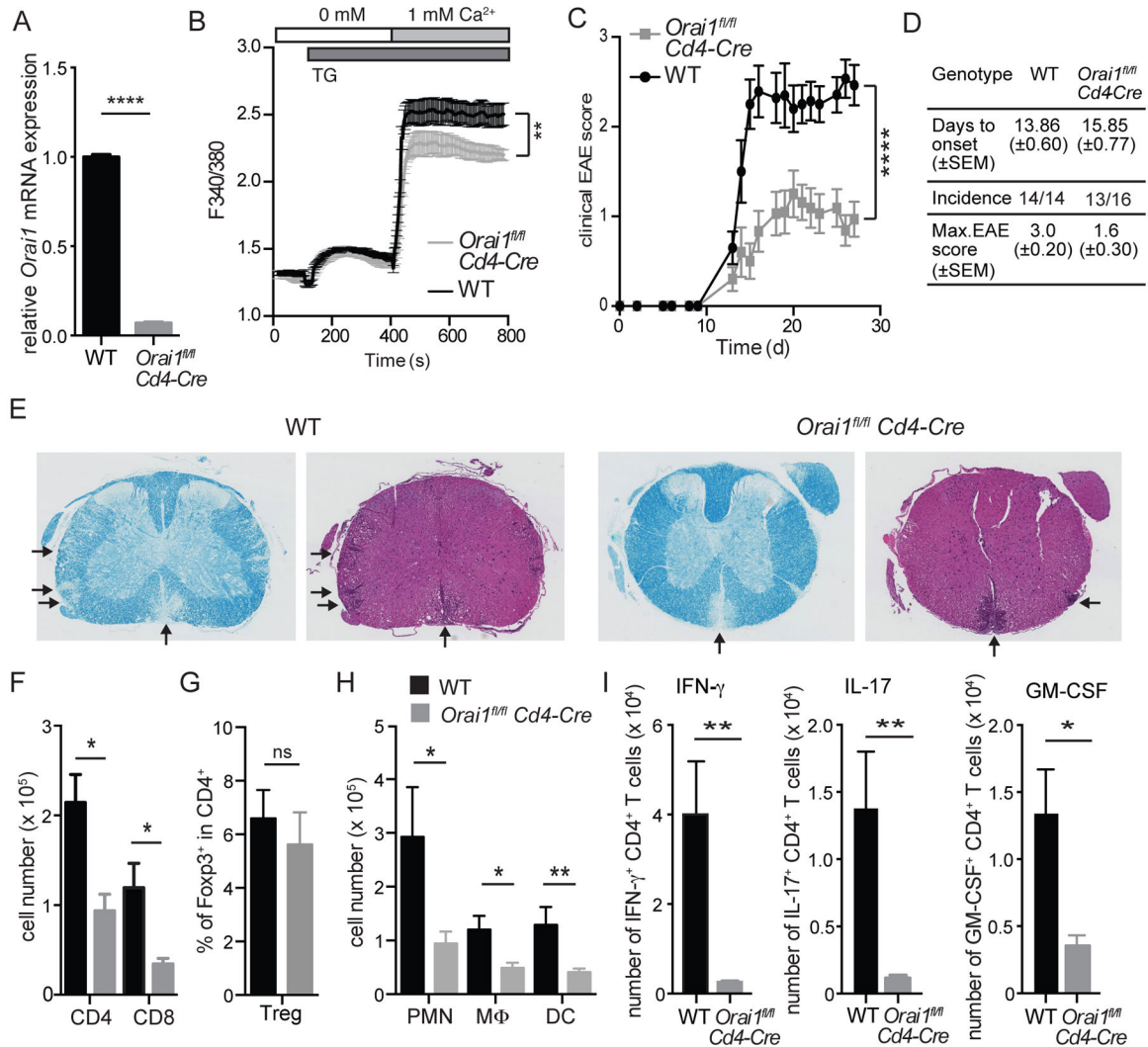


Figure 1. Experimental autoimmune encephalomyelitis (EAE) is ameliorated in *Orai1^{fl/fl} Cd4-Cre* mice

(A) RNA from wildtype and *Orai1^{fl/fl} Cd4-Cre* was isolated from CD4⁺ T cells and relative mRNA expression was measured by RT PCR. (B) SOCE was measured in Fura2-AM loaded freshly isolated CD4⁺ T cells from wildtype and *Orai1^{fl/fl} Cd4-Cre* mice after stimulation with thapsigargin (TG) followed by readdition of 1 mM Ca²⁺ to the extracellular medium. (C) Clinical EAE scores in WT and *Orai1^{fl/fl} Cd4-Cre* mice injected with MOG₃₅₋₅₅ in CFA. (D) Summary of EAE with days to onset (±SEM), incidence of EAE and maximal EAE scores (±SEM). (E) H&E and Luxol fast blue staining of spinal cords from WT and *Orai1^{fl/fl} Cd4-Cre* mice at 27 after EAE induction. Arrows indicate infiltrating cells and demyelination, respectively. Shown is one histological stain representative of 4 mice per group and 6 examined levels of spinal cord per mouse. (F–I) Cells were isolated from the spinal cord (CNS) of WT and *Orai1^{fl/fl} Cd4-Cre* mice at day 27 after EAE induction and analyzed by flow cytometry. (F–H) Absolute numbers of CD4⁺ and CD8⁺ T cells (F), frequencies of Foxp3⁺ CD4⁺ T cells (G) and absolute numbers of CD11b⁺ Gr-1⁺ polymorphonuclear cells (PMN), CD11b⁺ CD11c⁻ Gr-1⁻ macrophages and CD11c⁺ Gr-1⁻

dendritic cells in the CNS (**H**). (**I**) Cytokine production of T cells isolated from the CNS was analyzed by flow cytometry after stimulation with PMA and ionomycin in the presence of Brefeldin A for 6 h. Shown are absolute numbers of CD4⁺ T cells expressing IFN- γ , IL-17 or GM-CSF. Data in panels A and B represent the average \pm SEM of 3 mice per group. Data in panels C–D and F–H represent the average \pm SEM of 14–16 mice per group. Statistical analysis of EAE scores (starting at the first clinical signs of EAE) was performed using a Mann-Whitney test (panel C); data in panels B, F–H were analyzed using an unpaired Student's t test. * $p < 0.01$, ** $p < 0.001$.

Author Manuscript

Author Manuscript

Author Manuscript

Author Manuscript

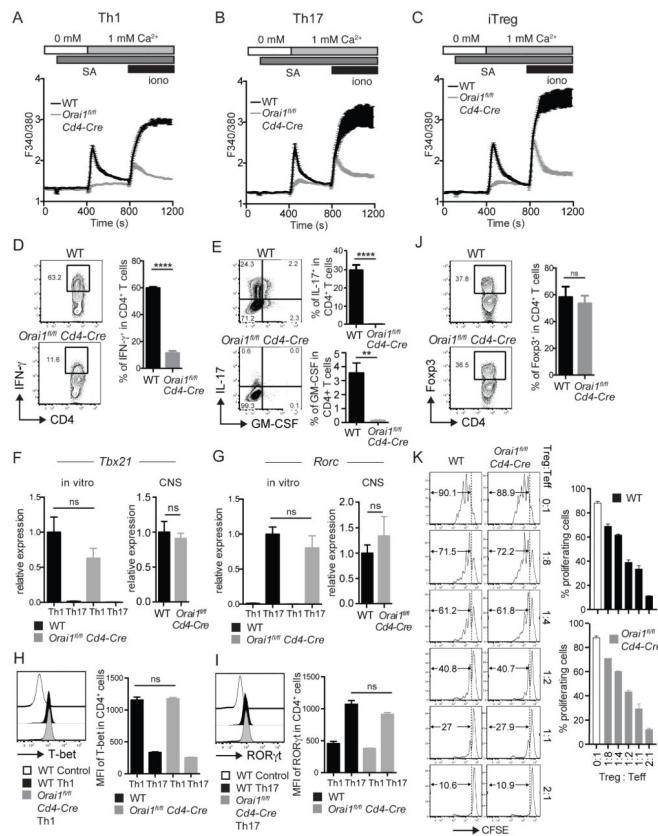


Figure 2. Lack of ORAI1 attenuates SOCE and severely inhibits the function of Th1 and Th17 but not iTreg cells

Naïve CD4⁺ T cells from spleen and LNs of WT and *Orai1^{fl/fl} Cd4-Cre* mice were stimulated with anti-CD3/CD28 and cultured for 3 days in vitro under Th1, Th17 and iTreg polarizing conditions. (A–C) SOCE was measured in Fura2-AM loaded cells after stimulation with anti-CD3-Biotin and crosslinking with streptavidin followed by readdition of 1 mM Ca²⁺ to the extracellular medium. (D, E) Frequencies of IFN- γ ⁺, IL-17⁺ and GM-CSF⁺ CD4⁺ T cells measured after stimulation with PMA and ionomycin for 6 h in the presence of Brefeldin A. Bar graphs represent the average \pm SEM from 4 independent experiments with one mouse per group. (F, G) Relative mRNA expression of *Tbx21* and *Rorc* in Th1 and Th17 cells cultured in vitro (left) and in lymphocytes isolated from the spinal cord of WT and *Orai1^{fl/fl} Cd4-Cre* mice on day 27 after immunization with MOG₃₅₋₅₅ peptide in CFA (right). *Tbx21* and *Rorc* mRNA levels were analyzed by real-time PCR (and normalized to Hprt1 (left panels) or CD4 in right panels). Bar graphs represent the average \pm SEM of 4–6 mice per group. (H, I) Flow cytometric analysis of T-bet and ROR γ t in Th1 and Th17 polarized cells. WT control in the left panel are Th17 polarized cells and WT control in the right panel are Th1 polarized cells. Bar graphs represent the average \pm SEM from 3 mice per group. (J) Frequencies of Fcpx3⁺ CD4⁺ iTreg cells after 3 days in vitro without restimulation. Bar graphs represent the average \pm SEM from 4 independent experiments with one mouse per group. (K) ORAI1 is not required for iTreg function. WT or *Orai1^{fl/fl} Cd4-Cre* iTreg cells that had been differentiated for 3 days in vitro were coincubated at different ratios with CFSE-labeled, anti-CD3-stimulated CD4⁺ T cells and

splenocytes from WT mice. Proliferation of CD4⁺ T cells was assessed after 3 days in culture by CFSE dilution and flow cytometry. Shown is one representative experiment done in triplicates of two independent experiments. No statistically significant difference of proliferation was detected between T cells incubated with WT and *Orail*-deficient Treg cells at different ratios by one-way ANOVA. Statistical analysis in D-J was performed using an unpaired Student's t test. ** p < 0.01, **** p < 0.0001.

Author Manuscript

Author Manuscript

Author Manuscript

Author Manuscript

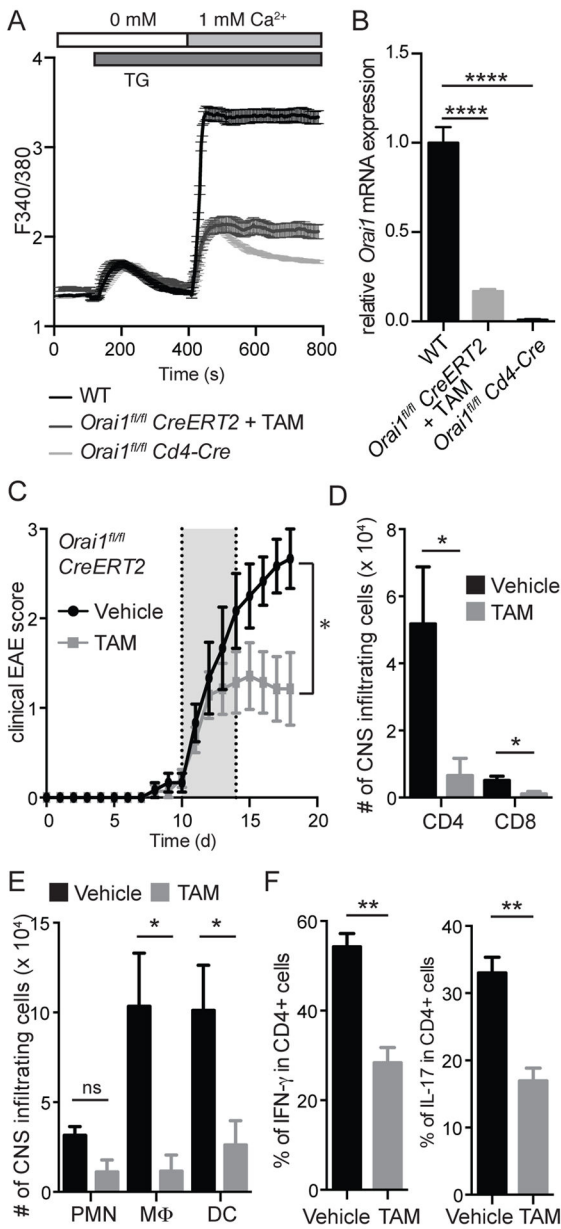


Figure 3. Inducible deletion of *Orail* gene in T cells during ongoing EAE ameliorates disease severity

(A,B) In vitro deletion of *Orail* in CD4⁺ T cells isolated from *Orail^{fl/fl} Cre-ERT2*, WT and *Orail^{fl/fl} Cd4-Cre* control mice. Cells were stimulated with anti-CD3/CD28 for 3 days in the presence of 1 μM tamoxifen (TAM) and analyzed for SOCE after stimulation with thapsigargin and addition of 1 mM Ca²⁺ (A) and *Orail* mRNA expression by RT PCR (B). (C–F) For passive induction of EAE, *Orail^{fl/fl} Cre-ERT2* and WT mice were immunized with MOG peptide. T cells were isolated from spleen and LNs 12 days later and restimulated in vitro with MOG peptide in the presence of IL-23 for 3 days. 4 × 10⁶ CD4⁺ T cells were transferred i.v. into sublethally irradiated CD45.1 recipient mice. After EAE symptoms developed, recipient mice were injected with tamoxifen or vehicle control from

day 10–14 after T cell transfer. (C) Clinical EAE scores. (D–F) Absolute numbers of CD4⁺ and CD8⁺ T cells (D) as well as CD11b⁺ Gr-1⁺ polymorphonuclear cells (PMN), CD11b⁺ CD11c⁻ Gr-1⁻ macrophages and CD11c⁺ Gr-1⁻ dendritic cells (E) in the CNS 18 days after adoptive transfer. (F) Frequencies of CD4⁺ IFN- γ ⁺ and CD4⁺ IL-17⁺ T cells isolated from the CNS and restimulated in vitro with PMA and ionomycin for 6h. Data represent the average \pm SEM of 3–4 mice per group. Statistical analysis of *Orail* expression in B was performed using a one-way ANOVA test. Statistical analysis of EAE scores (days 10–18) in C was performed using a Mann-Whitney test. Data in panels D–F were analyzed using an unpaired Student's t test. * p < 0.05, ** p < 0.005, **** p < 0.0001.

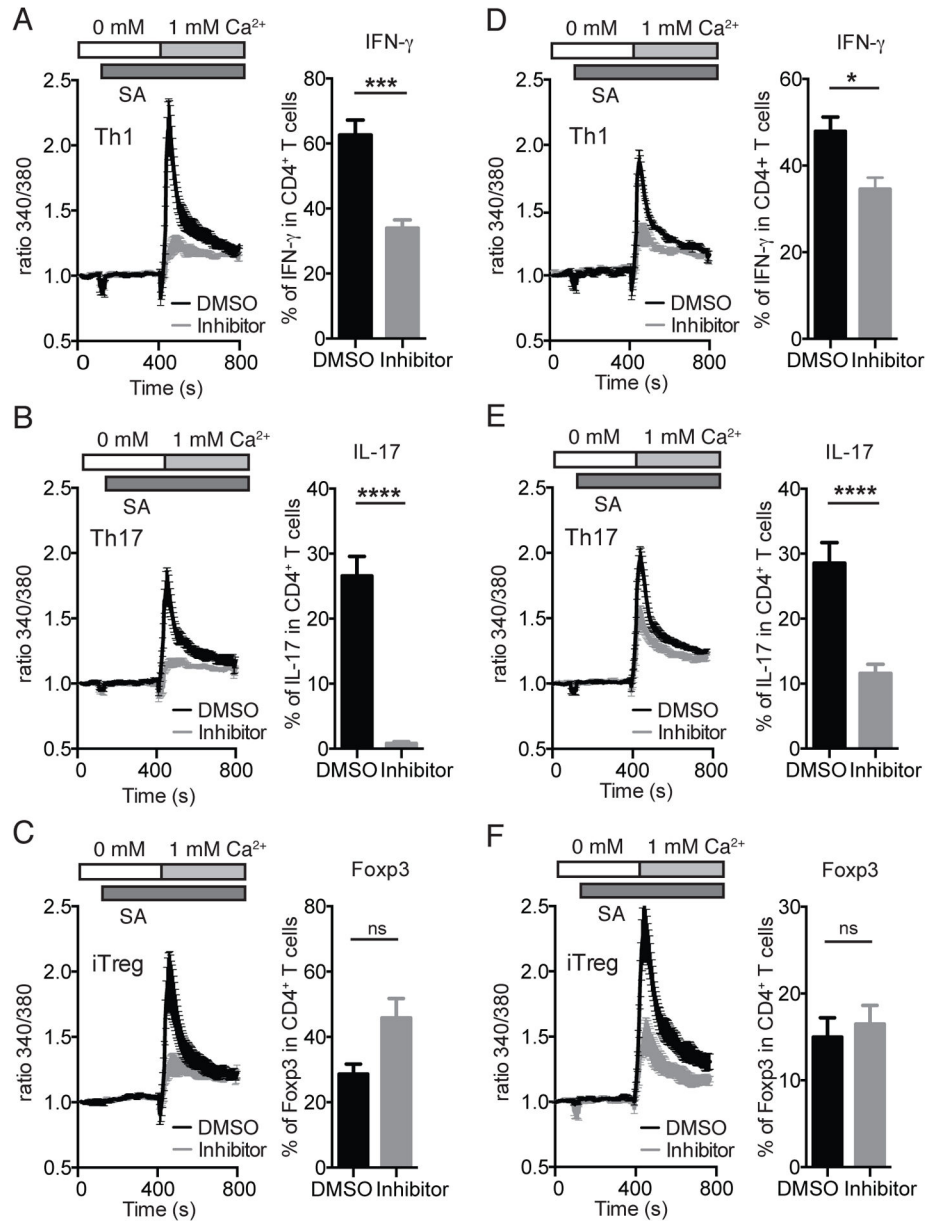


Figure 4. The function of Th1 and Th17 but not iTreg cells is blocked by selective CRAC channel inhibitor

CD4⁺ T cells isolated from the spleen and LNs of WT were stimulated with anti-CD3/CD28 for 3 days in vitro under Th1, Th17 and iTreg polarizing conditions. The CRAC channel inhibitor AMG1 (100 nM) or vehicle (DMSO) was added on day 0 and was present throughout T cell differentiation (day 0–3) (A–C) or added on day 3 immediately before Ca²⁺ measurements (D–F, left panels) or restimulation to measure cytokine production (D–F, right panels). For Ca²⁺ measurements (left panels), CD4⁺ T cells were loaded with Fura2-AM, incubated with Biotin-labeled anti-CD3 and activated by CD3 crosslinking with streptavidin in Ca²⁺ free extracellular buffer. To induce SOCE, extracellular [Ca²⁺] was raised to 1 mM. For cytokine production, CD4⁺ T cells were stimulated with PMA and

ionomycin for 6 h. For analysis of Foxp3 expression, CD4⁺ T cells were left unstimulated. Data represent the average \pm SEM of 3–8 mice per group. Statistical analysis was performed using an unpaired Student's t test. * $p < 0.05$, ** $p < 0.01$, *** $p < 0.0005$, **** $p < 0.0001$.

Author Manuscript

Author Manuscript

Author Manuscript

Author Manuscript

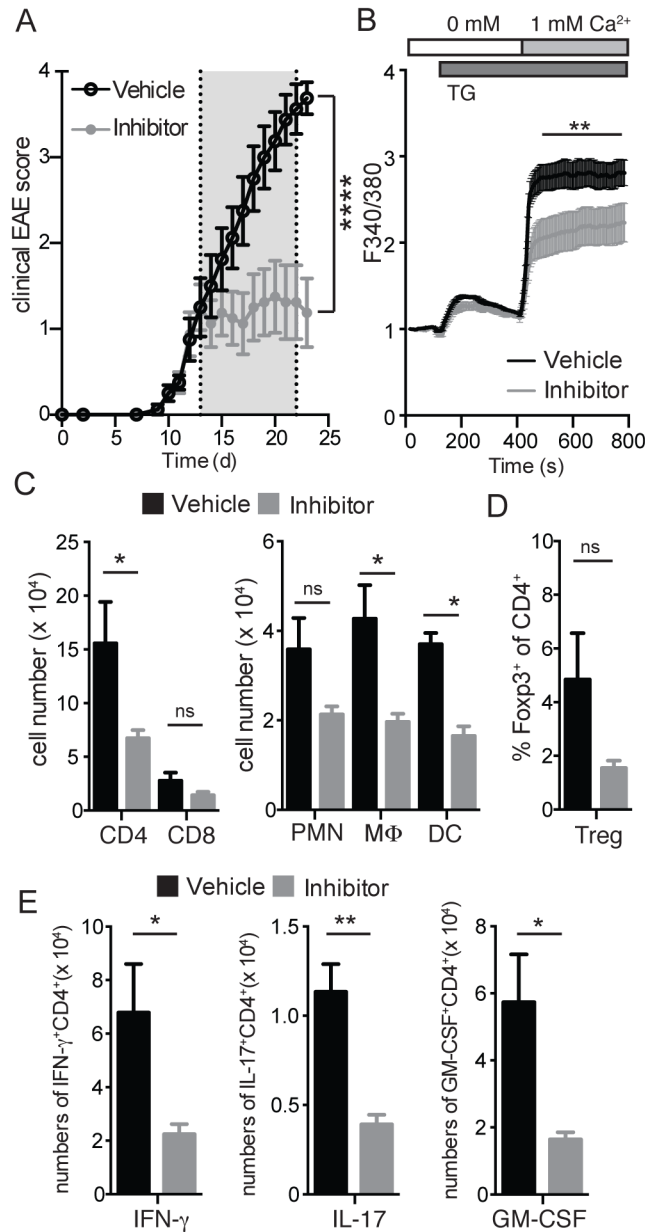


Figure 5. Progression and severity of EAE are attenuated by treatment of mice with CRAC channel inhibitor

(A) Clinical EAE score in WT mice injected with MOG₃₅₋₅₅ in CFA. Mice were treated with 6 mg/kg of the CRAC channel inhibitor AMG1 or vehicle control for 10 days starting when EAE scores were 1. Graphs represent the average \pm SEM of 8 mice per group. (B) Ca²⁺ influx was measured in splenocytes isolated at the end of 10 day treatment with inhibitor or vehicle. Cells were loaded with Fura2-AM and stimulated with 1 μ M thapsigargin (TG) in Ca²⁺ free buffer, followed by readdition of 1 mM extracellular Ca²⁺ to induce SOCE. (C) Absolute numbers of CD4⁺ and CD8⁺ T cells and CD11b⁺ Gr-1⁺ polymorphonuclear (PMN) cells, CD11b⁺ CD11c⁻ Gr-1⁻ macrophages and CD11c⁺ Gr-1⁻ DC isolated from the CNS of mice at day 23 after EAE induction and analyzed by flow

cytometry. **(D)** Frequencies of CD4⁺Foxp3⁺ Treg cells in the CNS at day 23 after EAE induction. **(E)** Expression of IFN- γ , IL-17 and GM-CSF by CD4⁺ T cells isolated from the CNS at day 23 after EAE induction and stimulated with PMA and ionomycin for 6 h. Data represent the average \pm SEM of 8 mice per group. Statistical analysis of EAE scores in A (days 13–23) was performed using a Mann-Whitney test; data in panels B–E were analyzed using an unpaired Student's t test. * $p < 0.01$, ** $p < 0.001$.

Author Manuscript

Author Manuscript

Author Manuscript

Author Manuscript

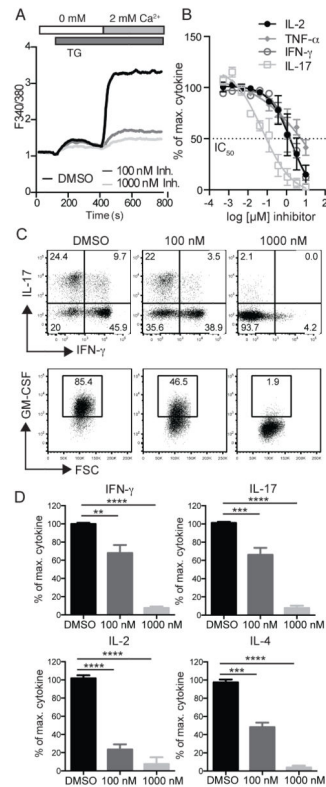


Figure 6. Suppression of SOCE and cytokine production in human T cells by CRAC channel inhibitor

(A) Human CD4⁺ T cells from healthy donors were cultured for 12 days in vitro and following incubated with 100 nM and 1000 nM of AMG1 for 2 h and analyzed for SOCE by stimulation with 1 μM Thapsigargin. Ca²⁺ traces are representative of 3 repeat experiments. (B) Human whole blood from healthy donors was treated with different concentrations of AMG1 (0.5 nM – 10 μM) and analyzed for cytokine production by immunoassay after 24 h stimulation with PMA and ionomycin. Data represent the average ± SEM of 2 experiments. (C, D) Sorted human CD4⁺ CCR6⁺ T cells from a healthy donor were stimulated with anti-CD3/CD28 coated beads and expanded in IL-2 containing medium for 12 days. Cells were treated with 100 nM and 1000 nM of AMG1 1 h before and during restimulation with PMA and ionomycin for 4 h in the presence of GolgiStop. Cytokine expression was analyzed in CD4⁺ CCR6⁺ T cells by flow cytometry. Data in D represent the average ± SEM of 4 repeat experiments. Statistical analysis of data in D was performed using one-way ANOVA test. ** p < 0.005, *** p < 0.001, **** p < 0.0001.